Master Thesis

ESTIMATING POPULATION ABUNDANCE OF FIRE SALAMANDER LARVAE OVER ONE BREEDING SEASON

Michèle Reich

January 2021

Supervision by:

Dr. Benedikt Schmidt

Prof. Dr. Arpat Ozgul

Department of Evolutionary Biology and Environmental Studies,

University of Zurich

Zusammenfassung

Der globale Rückgang der Biodiversität beschäftigt die Naturschutzbiologie seit nun einigen Jahrzehnten. Die Amphibien sind ein Beispiel für einen solchen Populationsrückgang des Anthropozäns. Es wird geschätzt, dass rund 43.2% aller Amphibien weltweit in irgendeiner Weise einen solchen Populationsrückgang erfahren. Diese werden meist ausgelöst durch eine Kombination von mehreren Stressfaktoren, die sich durch ein Zusammenspiel verstärken und die Lebensfähigkeit einer Population beeinflussen. Ein Populationsrückgang hängt jedoch immer mit der Demographie zusammen und dies unabhängig von den kausalen Faktoren. Wenn sich eine Demographie von ihrem Normalzustand wegbewegt, kann dies in einem Rückgang der Population resultieren. Eine wichtige Grundlage in der Naturschutzbiologie ist das Wissen wie eine Population funktioniert, um sie so effektiv zu schützen. Daher ist die Kenntnis über die Demographie, sowie den Stressfaktoren die diese verändert, grundlegend. Bei Amphibien wissen wir sehr viel über deren Demographie, jedoch nicht über das Larvenstadium. Eine dieser Amphibienarten ist der Feuersalamander (*Salamandra salamandra*). Er wurde zuletzt im Jahre 2005 auf der Roten Liste der Schweiz als «bedroht» klassifiziert und ist betroffen von einem weitergehenden Populationsrückgang. Diese Arbeit beschäftigt sich mit Umweltfaktoren, welche einen Einfluss auf das Wachstum einer Larvenpopulation haben können. Sie soll dazu dienen, ein besseres Verständnis über das larvale Stadium des Feuersalamanders zu gewinnen. Als Alternative zu der Fang-Wiederfangmethode, in welcher Individuen markiert werden müssen, wurde hier als Alternative eine nicht-invasive Methode mit wiederholten Zählungen angewandt. Dazu wurden 120 natürlich vorkommende Pools in vier Bächen einmal in der Woche und zweimal pro Tag ausgezählt über einen Zeitraum von 11 Wochen, beginnend Mitte April bis Anfang Juli. Dies ist die Hauptablegezeit von Larven der Feuersalamander-Weibchen. Gemessene Umweltfaktoren waren Regenmenge und Poolgrösse (gemessen an der mittleren Tiefe des Pools). Die Abundanzen, sowie auch deren Wachstumsraten wurden mit Hilfe eines N-mixture Modells für jeden Bach separat geschätzt, da die Bäche sehr unterschiedliche Verlaufsmuster über die Zeit aufzeigten. Die Resultate meiner Analyse zeigten, dass das beste Modell für jeden Bach unterschiedlich ist. Das bedeutet, dass nicht in jedem Bach die gleichen Einflussfaktoren eine Larvenpopulation (hier definiert als alle Larven lebend in einem Pool) beeinflussen. Während die Anfangsabundanz nicht beeinflusst wird von der Poolgrösse, zeigt sich über die Zeit eine erhöhte Wachstumsrate in tieferen Pools. Eine steigende Wassertemperatur, sowie eine erhöhte Regenmenge und ein späterer Zeitpunkt in der Beobachtung erniedrigt die Wachstumsrate einer Larvenpopulation. Ein positiver Effekt von Regen in tieferen Pools konnte jedoch in einem Bach gefunden werden. Obwohl gewisse Faktoren wie Temperatur

und Pooltiefe vermehrt vorkommen, zeigen die Resultate klar, dass jeder Bach laut Modell andere Einflussfaktoren hat, welche das Wachstum einer Population beeinflussen. Ein Schutz des larvalen Stadiums ist sehr komplex, da jeder Bach je nach Struktur und Ort von unterschiedlichen Faktoren beeinflusst wird. Trotzdem lässt sich sagen, dass für den Schutz des Larvenstadiums vor allem tiefere Pools, sowie eine niedrigere Temperatur wichtig sind, da sie zu einer höheren Wachstumsrate einer Larvenpopulation führen. Um dies zu erreichen ist vor allem der Erhalt eines natürlichen Bachverlaufs (keine Begradigungen oder Verflachungen des Bachs) und ein belassen des umliegenden Waldes von grosser Wichtigkeit.

Abstract

The use of quantitative methods in conservation biology can lead to more efficient species protection. It is estimated that at least 43.2% of amphibians are experiencing some form of population decrease, serving as an example of the biodiversity loss in the Anthropocene. Population declines generally emerge from a shift in demography independently of the underlying causal factors. For a better understanding of a population's dynamic, knowledge about demography and stressors affecting it is crucial. In amphibians, as for instance salamanders, there is not much information on larval stages under natural conditions. Thus, in this field study, I estimated the larval abundance of the fire salamander in four different streams in relation to different environmental factors, among them rainfall, pool size and water temperature. For this, a non-invasive method (i.e., replicated counts) was used as an alternative to marking. For 11 weeks, i.e., most of the larval period, I recorded replicated larval counts of 120 distinct pools every week. An open N-mixture model was applied to each stream separately, which estimates abundance and growth rate, as well as detection parameters. The best model differed between the streams, indicating environmental factors to have different influences on larval populations. Deeper pools as well as early date in the season revealed a higher larval growth rate. Water temperature and rain affected larval growth rate negatively. Interestingly, in deeper pools (20 cm pool depth), higher rainfall led to a higher growth rate. The positive impacts of larger pool depths on growth rate can be explained by a lower flush out effect and a slower warming thereof. Water temperature and its negative effects could be diminished by a streamside forest. Management strategies such as a regulation of deforestation near fire salamander habitats and stream preservation in their natural flow (and especially pool depth) are of high importance.

Keywords

fire salamander, *Salamandra salamandra terrestris*, amphibians, population decline, Switzerland, conservation biology, estimation of population abundance, open population model

Contents

1 Introduction

The use of quantitative methods in conservation biology can lead to more efficient species protection by prioritizing research, planning species protection and monitoring management efforts (Benton & Grant, 1999; Biek et al., 2002). Nowadays, the worldwide continuing biodiversity loss is a major challenge in conservation biology (Hoffmann et al., 2010; Stuart et al., 2004). It is estimated that one-fifth of the world's vertebrates are threatened, whereas in amphibians it is estimated that at least 43.2% are experiencing some form of population decrease (Hoffmann et al., 2010; Stuart et al., 2004). Population declines are thought to be the result of complex interactions among multiple stressors that often act synergistically (Blaustein & Kiesecker, 2002), making their recognition challenging. Nevertheless, declines are always, regardless the underlying causal factors, in connection with the demography of a population. When a demography shifts away from its normal state, it can result in a population decline. This is not unique to amphibians, as it has been shown in several studies concerning mammals (Ferreira et al., 2015) and reptiles (Dorcas et al., 2007), where a decline in population was due to a demographic shift. The environment (e.g., weather) can affect parameters such as number of births and deaths. Warmer temperatures have shown to alter the behaviour of amphibians (i.e., movement, dispersal) (Blaustein et al., 2010), such as a tendency of earlier breeding in anurans (Beebee, 1995). Heavy rainfall has been shown to negatively affect larval survival in salamanders by reducing larvae living in a stream (Baumgartner et al., 1999). An important foundation in conservation biology is knowing how populations function and how vital rates vary under natural conditions, in order to protect it effectively (Benton & Grant, 1999; Govindarajulu & Anholt, 2006). Therefore, knowledge of demography, as well as stressors that influence it, is fundamental. In amphibians, we know a lot about their demography, but not about the larval stage. However, this knowledge would be useful if we want to apply the modern quantitative approach in species protection and henceforth, estimations of vital rates are needed for rare specialists as well as for more common species, such as amphibians, since they are declining rapidly (Petrovan & Schmidt, 2016). A recent review of Petrovan & Schmidt (2019) found divergent findings in literature about the importance of a stage of a specific species. The view of larval stages (i.e., survival of pre-metamorphic animals to metamorphosis) has been found to be contributing the most to a population's dynamic in a few studies (e.g., Beebee et al. (1996); Jones et al. (2017); Semlitsch (2000)), whereas Petrovan & Schmidt (2019) concluded the juvenile stage as most critical in many amphibian species. Despite this, it does not imply that other stages are not important to assess and conservation strategies of the larval stage that lead to a larger juveniles could even increase the viability thereof (Schmidt, 2011).

One of these amphibians affected by a population decline is the fire salamander (*Salamandra salamandra*). The fire salamander exhibits a complex life cycle (CLC; i.e., species having a larval and adult stage) and inhabits the aquatic as well as the terrestrial habitat at different stages of its life (Semlitsch, 2000; Thiesmeier, 1992). This makes it susceptible to a wide range of various environmental stressors (Manenti et al., 2009). Especially the larval stage of the fire salamander is still poorly observed and to better assess it, reliable information of vital rates (e.g., survival) under natural conditions are needed (Govindarajulu & Anholt, 2006). Most studies concerning the larval stage focus on presence-absence data (e.g., Sandvoß et al. (2020)) or yearly count data (e.g., Wagner, Lötters, et al. (2020)) to record the occurrence or yearly abundance of larvae. But for conservation, there is also an urgent need in identifying factors that underly different growth rates of larval populations and hence having data on vital rates as well as on factors affecting these. While data on larval abundance trends over one breeding season remain scarce, they show, if available, a high dependency on a temporal and spatial scale (e.g., Hannappel & Schiefenhövel (2013)). This is because in amphibians, population fluctuations over time are a common pattern (Pechmann & Wilbur, 1994) and the abundance of amphibians varies naturally from region to region. Therefore, findings in such studies cannot be generally applied to just any other fire salamander population. Analysing the change in abundance can help us in better understanding the dynamics of a larval population. Moreover, growth rates or their deviated survival rates can be used to complement knowledge about the importance of the larval stage to the population's dynamic (Govindarajulu & Anholt, 2006). Previous studies have highlighted the importance of several habitat features such as forest cover (Manenti et al., 2009), number of pools in a stream (Schmidt et al., 2015) or elevation (Wagner, Harms, et al., 2020) on fire salamander abundance. Nevertheless, it is not known how these factors affect the change in larval abundance over a breeding season.

Here, I estimated the larval abundance of the fire salamander (*Salamandra salamandra terrestris*), as well as their growth rates depending on different environmental factors. While capture-mark-recapture (CMR) methods rely on marking, i.e., photos in adults or special fluorescent tags in larvae (e.g., Wagner, Pfrommer, & Veith (2020)), this field study used replicated counts, a non-invasive method, as an alternative. A reoccurring approach in literature is to observe stream sections with a certain length (Segev & Blaustein, 2014; Wagner, Lötters, et al., 2020), whereas this study rather focused on following larvae living in 130 distinct pools. I aimed to (i) estimate the larval abundance and (ii) identify environmental factors that influence growth rate of a population over one breeding season.

2 Methods

2.1 Study area

For this study, I surveyed five streams located in the canton of Basel-Landschaft (BL, Switzerland) (Figure 1). These five streams are all situated close to Sissach and hereafter named by the streams they are flowing into or their surrounding area since these streams are rather small and therefore do not have own names. The following names were given: Diegterbach (N 47.424667, E 7.821500), Chrintelbach (N 47.4363611, E 7.8558056), Buechmatt (N 47.434850, E 7.825600), Binzholdengraben (N 47.507130, E 7.853650) and Talbächli (N 47.454470, E 7.785584). Weather data were taken from a weather station located in Rünenberg (RUE, 613 MSL) (Data were provided by the Federal Office of Meteorology and Climatology (MeteoSwiss, 2020)).

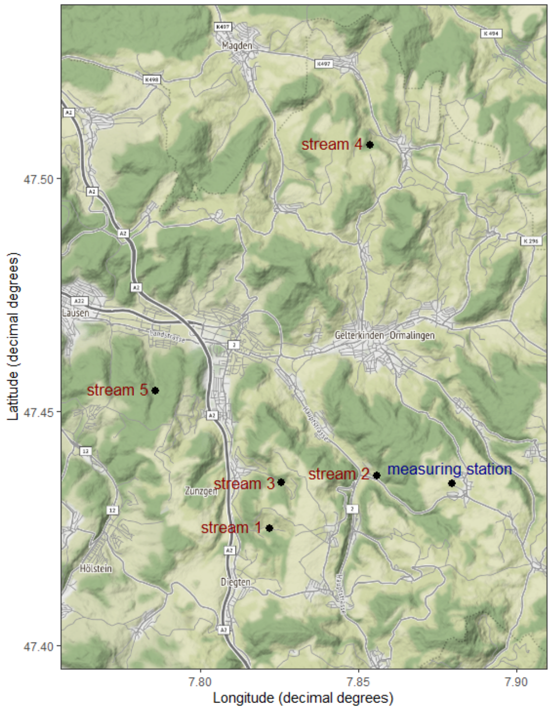

Figure 1: Locations of the five streams and the weather station. Stream 1: Diegterbach, stream 2: Chrintelbach, stream 3: Buechmatt, stream 4: Binzholdengraben and stream 5: Talbächli.

2.2 Study species

The fire salamander (*Salamandra salamandra*) is widely distributed throughout central and southern Europe to northern Africa and the Middle East (Thiesmeier, 1992). It was last classified as vulnerable in 2005 on the Red List of threatened species in Switzerland

(Schmidt & Zumbach, 2005). Its preferred habitat is a humid mixed deciduous and coniferous forest with spawning waters or streams to deposit the larvae (Thiesmeier, 1992). The fire salamander shows an annual seasonal reproduction (Duellman & Trueb, 1994). Fertilization of most salamanders takes place either external or through oviposition, whereas the fire salamander female can store spermatozoa in the spermatheca from autumn, when mating occurs, until the following spring (Duellman & Trueb, 1994). Females deposit their larvae into a water body, preferably a stream, across a period that varies between beginning of March until mid May, exhibiting a lecithotrophic viviparity (i.e., giving birth to larvae without maternal provisioning) (Cayuela et al., 2019; Thiesmeier, 1992). The deposition of larvae is initiated by increasing temperatures, spring rains and water saturation of the ground by melting snow (Duellman & Trueb, 1994; Thiesmeier, 1992). A larva spends between three to five months in a water body until metamorphosis (Thiesmeier, 1992). After metamorphosis, it enters the juvenile stage and leaves the water to live in the terrestrial habitat. It comes back to the aquatic habitat, when sexual maturity is reached (after 2-4 years) to deposit its own larvae (Thiesmeier, 1992). Salamanders exhibit a slow life-history strategy (i.e., low annual fecundity and high adult survival) and have therefore a long life expectancy (Cayuela et al., 2019).

2.3 Study design and data collection

2.3.1 Stream properties

Each stream was surrounded by a mixed deciduous forest, with a forest coverage of ~ 50% - 100% (in a 200 m radius), and had at least 30 natural pools in the streambed (Table 1). These were typically between 2 and 4 meters apart from each other. With an increasing number of pools and riffles (i.e., shallow and low flowing parts of a river) the stream heterogeneity also increases (Manenti et al., 2009). Present riffles and pools, consisting of leaves and stones, provide hiding places for fire salamander larvae. These play an important role to avoid drift, especially for younger larvae (Manenti et al., 2009), and are their preferred habitat. Furthermore, a low stream velocity (threshold of < 0.27 m/s suggested by Segev & Blaustein (2014)), minimizes the effect of larval drift due to the ability of the larvae to actively resist entering drift. I selected the five streams based on these two main criteria, as well as the presence of larvae established with a preliminary field survey. Additionally, streams can be categorized into first and second order streams (a method developed by Strahler (1957)). All of the streams were first-order streams, with exception of Chrintelbach, which was a second order stream (Table 1). Nevertheless, all streams were similar in their size and stream velocity. There were similarities and differences between streams, as forest coverage, usage and the water source (Table 1).

Table 1: Characteristics of the five streams.

stream	stream order	forest coverage [%] (200 m radius)	usage	water source
DI	first	50.78	agriculture	rain
CH	second	87.48	forest	rain
BU	first	73.83	agriculture	spring
BI	first	79.04	forest	spring
TA	first	100.00	forest	spring

Note: A first order stream is defined as the smallest tributary of a drainage basin and a second order stream is formed when two first-order channels converge (Strahler, 1957). The following abbreviations were used: DI = Diegterbach, CH = Chrintelbach, BU = Buechmatt, BI = Binzholdengraben and TA = Talbächli.

2.3.2 Field methods

The fieldwork was conducted from mid-March to the beginning of July 2020 for 15 weeks. I chose this timespan due to the annual reproduction pattern of fire salamanders. Simulations by Kéry & Royle (2016) suggested a replication minimum of 20 sites and a temporal replication of two or more per site. Therefore, I divided each stream into 30 pools (30 spatial replications, total of 150 pools), which I observed once per week and twice per day (two temporal replications). In each pool, I searched for larvae for four minutes with a twig. Each observation was conducted from downstream to upstream to avoid turbidity and keep the water clear. I tried to avoid stepping into the water as much as possible, trying not to disturb the larvae in their natural habitat. This is of importance because the two temporal replications represent a closed population (i.e., no drifts or deaths).

2.3.3 Measurements

I evaluated the following environmental factors: forest coverage, usage, creek order, water source (Table 1) and rain. Forest coverage was measured within a radius of 200 m from the middle of the observed section with ImageJ (ImageJ 1.53c, Schindelin et al. (2012)). Usage was assigned on site to either forest or agriculture by looking at the surrounding area. Creek order and water source were evaluated with Google Maps (GoogleMaps, 2020). Rain data were taken from the weather station in Rünenberg (Figure 1). This data was provided in the amount [mm] it rained in one day (MeteoSwiss, 2020). I used this data to create three different categories of rainfall. For a short-term influence, rain measurement was taken the day before observation, for a mid-term influence the last three days before observation were summed up and for a long-term influence the last seven days of rain before observation were summed up. Furthermore, I measured the above-ground and water temperature at each observation time point in each pool. To correct for the differences in pool size, I took different measurements of pool size. I measured the maximum pool depth at the deepest point of the pool and for the mean pool depth I calculated the mean from five distinct points in a pool (Table 2). Lastly, I measured pool width and pool length. These pool measurements were taken all four weeks (i.e., three times over the whole study). Per pool, a mean of all three measurements was calculated for the later analysis.

Potential factors that affect the results

There were several factors that the larval counts could potentially have been affected by. One factor of these factors is the weather. After rainfall the day before observation, the water could have been turbid. Furthermore, the stream velocity was higher and the reflection on the water surface was stronger, which made it more difficult to see them. The former and the latter can affect the sight and therefore the detection probability. Another factor is a potential misidentification of the species. Since the alpine newt (*Ichthyosaura alpestris*) was also present in several streams (especially in Chrintelbach), there could have occurred a misidentification between these larvae. This could especially have been a problem in deeper pools or turbid water, where larvae were not well visible. The larval abundance would have been overestimated in this case.

2.4 Statistical analysis

A recently extended and improved state-space model, the Dail-Madsen Model (DM model), estimates local abundance and detection parameters based on replicate observations (Hostetler & Chandler, 2015). The DM model is an open N-mixture model, which incorporates parameters describing the population change over time (Hostetler & Chandler, 2015). This approach allows a visual observation of the individuals, without the need of marking or taking out. It assumes demographic closure between two replicate observations, but allows the abundance to vary between sampling periods (i.e., between weeks). With a model extension for population growth, the DM model estimates the initial abundance, the finite rate of increase and the detection probability (Hostetler & Chandler, 2015).

The population size ($N_{i,t}$) for site i at time t can be modelled as followed:

$$N_{i,t} \sim Pois(exp(r) N_{i,t\text{-}1}). \tag{1}$$

The observation process (Equation (2)) can be modelled with a binomial distribution (Dail & Madsen, 2011). The observed counts (y) result from the population size ($N_{i,t}$) described in equation (1) combined with the detection probability (Hostetler & Chandler, 2015).

$$y_{i,t} \sim Binomial(N_{i,t}, p) \tag{2}$$

I conducted the analysis in RStudio (R version 4.0.3, R Core Team (2020)). All streams were analysed separately, since they show a different pattern in their abundance over time. Therefore, site-specific variables that only differ between, but not within, streams (i.e., creek order, forest coverage, usage and water source) could not be included as covariates into the models. Covariates included in the models were: Rain, mean pool depth, water temperature and day (see Table 2 for their usage in the parts of the model).

Table 2: Abbreviations, descriptions and usage of the covariates in the models.

Abbreviation	Description	Initial abundance	Growth rate	Detection probability
rain24	Rain [mm] the day before observation			✓
rain7	Rain [mm] summed up for the last seven days before observation		✓	
pool_depth_mean	The mean pool depth of each pool taken at the uppermost, lowermost, rightmost, leftmost and the middle of the pool	✓	✓	✓
watertempmean	The mean of the water temperatures from two replicate observations		✓	
day	Number of days passed since start of the study		✓	✓

Note: Check marks explain, which covariates were included in the respective parts of the model (i.e., initial abundance, growth rate and detection probability). All covariates were then paired in each possible combination to build the models.

Since I took four different measurements of pool size that all intended to describe the pool's characteristics, only one of them was included into the models as a covariate, namely mean pool depth, to avoid multicollinearity. Mean pool depth correlated with the maximal pool depth, pool length and pool width (Spearman's rank correlation test: maximal pool depth $\rho = 0.96$, $p < 0.01$; pool length $\rho = 0.21$, $p = 0.01$ and pool width $\rho = 0.69$, $p < 0.01$). Larval count was considered as the response variable.

The variables water temperature, rain and mean pool depth were standardized prior to the analysis to a mean of zero and a standard deviation of one. An open N-mixture model was fitted for each stream using the 'pcountopen' function, whereas this and all further functions mentioned here are from the 'unmarked' package (Fiske & Chandler, 2011). The models were all fitted with a negative-binomial distribution. The upper boundary (K) (i.e., the truncation limit or summation limit of the likelihood) was set individually for each stream to ensure that there is no underestimation of the larval abundance (Appendix; Figure 6). Additionally, an immigration term was modelled to ensure a rescue of a population (i.e., when a population in one pool goes extinct, it can be recolonized either by drifts from upstream or births) (Kéry & Royle, 2020). A model ran typically about 5.5 hours, whereas a model without computing the standard errors (SEs) ran only about 3.3 hours. Thus, to improve the computational run time, models were run without calculating the SEs to compare their Akaike information criterion (AIC) (Kéry & Royle, 2020). Subsequently, the best models (Δ AIC to the highest ranking model ≤ 2) were run with computing the SEs.

For each part of the model (i.e., initial abundance, growth rate and detection probability), I built different N-mixture models with each combination of the four covariates as well as their interactions. First, the detection probability was modelled to determine which covariates best describe detection probability. Subsequently, the covariates best describing the detection probability were fixed to model the initial abundance. Thereafter, growth rate was modelled based on the best model from initial abundance. After each part, models were ranked by their AIC values using the 'modSel' function. The variables used as covariates, differed between the model parts (see Table 2 for abbreviations and combinations of the covariates in the different model parts). The amount of rain the day before observation was used as a covariate in the detection probability part of the model since it serves as a proxy for the influence of rain on a short term scale. Contrary, the sum of rain fallen in the last seven days before the observation day was taken in the growth rate part of the model because this is rather based on a long term scale. Hence, seven candidate models were fitted for detection probability, one model was fitted for initial abundance and 18 models were fitted for growth rate. Finally, a bootstrap goodness-of-fit (GOF) analysis was done with the 'parboot' function using three fit statistics (i.e., Sum of squared errors (SSE), Chi-squared test and Freeman-Tukey) (Kéry & Royle, 2020). These tests all look for a lack-of-fit evidence, therefore a p-value > 0.05 is a bad fit (Kéry & Royle, 2020). To estimate the site-specific abundances, the 'ranef' function was used.

One stream (Buechmatt) could not have been analysed due to the lack of finding an appropriate K for the model. One possibility is that the data were not appropriate for the model setting. The first four weeks had missing temperature data in all streams. Thus, I excluded the first four weeks and analysed only the last 11 weeks (hereafter named as week 1 to 11; starting from the 11th of April to the 3rd of July 2020). In the Chrintelbach, one pool had to be excluded due to its desiccation over the whole study period. Moreover, in Diegterbach, I observed an unusual high, but naturally occurring abundance over the whole study period in one pool (a biological outlier). This pool was excluded after comparing the GOF tests of the respective final models (with and without this outlier). The data with the outlier showed a lack-of-fit in two out of three GOF tests (SSE = 347'372 ± 82'245, $p < 0.05$; Chi-squared test: 8'009 ± 1'633, $p > 0.05$; Freeman-Tukey: 2'812 ± 648, $p < 0.05$), whereas the data without the outlier fitted the model better (SSE = 97'329 ± 21'532, $p > 0.05$; Chi-squared test: 4'598 ± 964, $p > 0.05$; Freeman-Tukey: 1'483 ± 278, $p > 0.05$). A GOF analysis (i.e., all three test statistics) resulted in a fitting model for each stream ($p > 0.05$).

3 Results

3.1 Detection probability

Analyses of the different covariates revealed that detection probability was affected by mean pool depth, day and rain. Mean pool depth positively correlated with the detection probability in all streams (Table 3). This covariate was significant in three out of the four models, indicating larger pool depths to lead to a higher detection of larvae. In two streams, the number of days passed since start of the observation led to a higher detection probability, whereas in one stream more days caused a decrease in detection (Table 3: DI, BI, TA). One model (Chrintelbach) did not include number of days passed in the best model. Nevertheless, the second best model (Δ AIC = 1.485; AIC weight = 0.2330) contains the variable "day" as well and hints on a positive correlation, even though it is not significant (Appendix; Table 5). This implies that with progressing time in the study, the detection probability becomes higher, which could be explained by the experience I collected over time. Finally, rain (the day before observation) was included in two models (Table 3: BI, TA). There were no significant effects of rain identified on detection probability. The amount of rain therefore had a low impact on detection probability.

3.2 Larval abundance

3.2.1 Raw data

Figure 2 shows the sum of larvae over all streams found per week. The first metamorphosing larva (i.e., yellow-black coloured larva) was detected in week one (Figure 2). Nevertheless, the occurrence of such larvae was rare during the first few weeks. Since the number of metamorphosing larvae was constant until week nine, it can be assumed that a decline in abundance was not due to larvae finishing metamorphosis with a subsequent leaving of the aquatic habitat. From week nine on, the metamorphosing larvae have increased by a factor of approximately three, and interpretations regarding growth rates should be treated with caution.

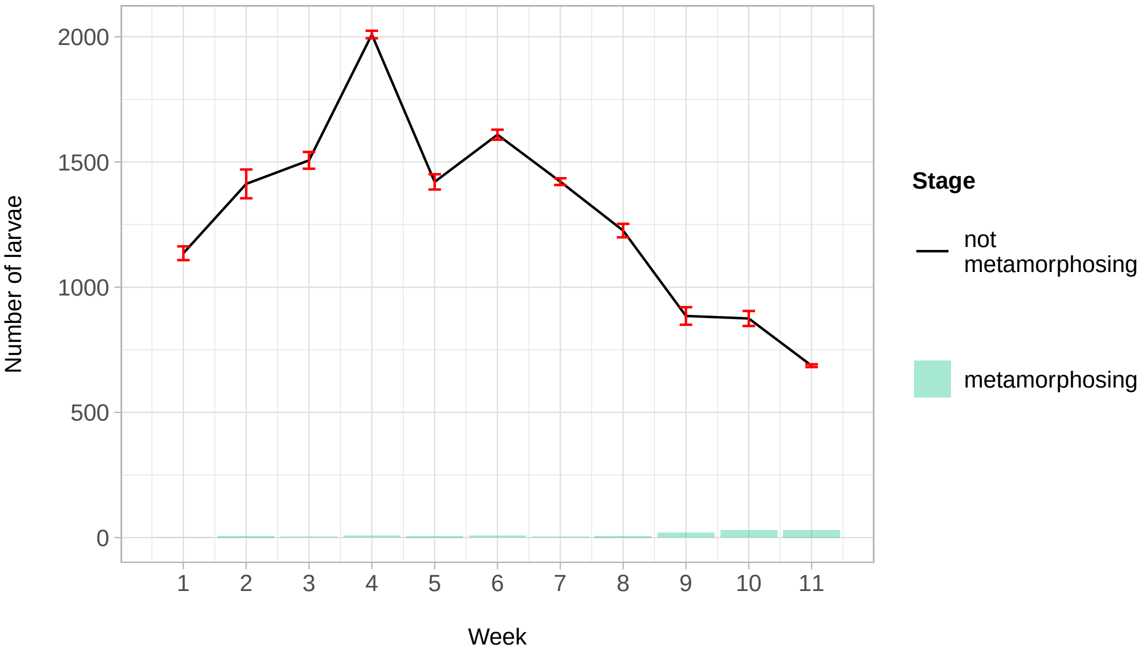

Figure 2: Sum of larvae over all streams per week presented as the mean between the first and second observation by a black line. Standard deviations are shown in red. The sum of the metamorphosing larvae found in all streams per week is indicated in lightgreen (highest number between first and second observation).

3.2.2 Model estimates

The larval abundance was estimated for 11 weeks. During this time the highest estimates were found in stream Binzholdengraben in week one (n = 2'540 larvae; mean = 84.7 ± 35.1 per pool; Figure 3). Also, this stream presented the lowest larval abundance in week 11 (total of 109 larvae; mean = 3.63 ± 2.93 per pool). When summed up over the whole study period, most larvae were found in Talbächli (n = 14’842 larvae; mean = 1’349 ± 282 per pool).

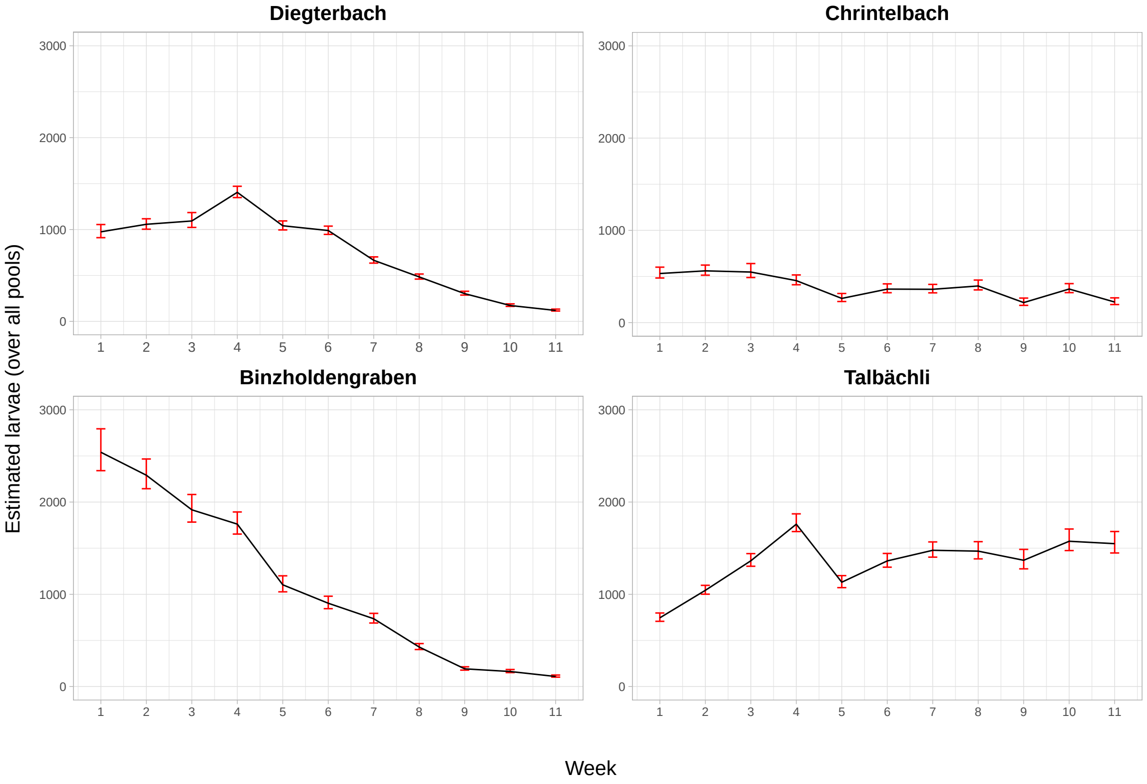

Figure 3: Larval abundance estimates depicted with a 95% confidence interval (CI) in red. Note that all pools from one stream are summarized per week.

Abundance estimates showed a remarkable variation among the four streams (Figure 3). Diegterbach displayed an increase in abundance until the fourth week where it reached its peak (n = 1’405 larvae; mean = 48.4 ± 30.5 per pool) and decreased constantly afterwards. The abundance in Chrintelbach remained low over the whole study period, exhibiting a fluctuating pattern with the highest larvae estimation of 561 larvae (mean = 19.3 larvae ± 9.31 per pool) in week two. Stream Binzholdengraben depicted a weekly decrease in abundance and in Talbächli the abundance increased until the fourth week with a total of 1’760 larvae (mean = 58.7 ±27.2), followed by a steep decrease in the fifth week down to 1’131 larvae and a steady increase from there onwards. A few pools in Chrintelbach dried out multiple times over the study period and were recolonized sometimes after pools were filled up with water again. Thus, the rather low abundance in this stream may have been caused by its low water income and low pool depths. The streams Binzholdengraben and Talbächli showed larger absolute abundance estimates than the other two streams. These differences may be due to different water incomes (Table 1). Streams with lower water income (only by rain) had smaller absolute abundances, whereas a constant water flow (spring) led to higher abundances. This finding is consistent with findings that state a positive impact of a permanent water flow (without drying out of stream sections) on larval density (Hannappel & Schiefenhövel, 2013).

3.3 Initial abundance

There was no covariate detected affecting the initial larval abundance (Table 3). This may have been caused by the model selection process. Due to modelling the detection probability first, covariates that already explain the detection probability sometimes do no longer explain the initial abundance. For instance, if mean pool depth is already explaining the detection probability, it will in some cases no longer explain the initial abundance. While if the initial abundance would have been modelled first, there could have been an effect of mean pool depth on it. This structure has been selected due to the fact, that we want to diminish the probability of pool depth having an effect on initial abundance when it would actually have an effect on detection probability. Nonetheless, in all streams the models with mean pool depth as covariate in the initial abundance part of the model revealed small AIC differences to the respective best model (Δ AIC ≤ 2, with AIC-weights of 0.27-0.37) (Appendix; Tables 4, 5, 6 and 7). These results indicate a potential influence of pool depth on initial abundance, even though not included in the final model.

3.4 Growth rate

Covariates affecting growth rate differed largely between streams. Water temperature was found to negatively affect growth rate in three models, while this was significant in two of them (Table 3: CH, BI, TA). Concluding, an increasing water temperature led to a decreasing population growth rate (Appendix; Figures 8, 9 a) and 10). Furthermore, mean pool depth occurred in two models out of the four, revealing a positive significant effect on growth rate (Table 3: DI, BI; Appendix; Figure 7 b) and 9 b)). This indicates that larger pool depths cause a higher survival. Rain was identified to negatively and significantly affect growth rate in one stream (Table 3: DI; Appendix; Figure 7 a)). As time progressed, the number of days passed had a negative and significant effect on growth rate in two models (Table 3: DI, BI; Appendix; Figure 7 c) and 9 c)). This may be caused to a certain extend by deaths or metamorphosis and a subsequent emigration out of the aquatic habitat, but mainly by deaths until the ninth week since metamorphosing larvae are constant.

Table 3: Covariates, estimates, standard errors (SE), AIC and AIC-weights (AICwt) of the best models (Δ AIC ≤ 2) for each stream.

Stream	Initial abundance	Growth rate			Detection probability			AIC	AICwt
		Variable	Estimate	SE	Variable	Estimate	SE		
DI	~1	~pool_depth_mean	0.0181*	0.0046	~pool_depth_mean	0.0051	0.1324	3167.14	0.72
		+ rain7	-0.0132*	0.0043	+ day	0.0260*	0.0073		
		+ day	-0.0017*	0.0003					
		+ pool_depth_mean : rain7	0.0099*	0.0040					
CH	~1	~watertempmean	-0.0159*	0.0079	~pool_depth_mean	0.8920*	0.1380	2140.48	0.25
	~1	~rain 7	-0.0048	0.0075	~pool_depth_mean	0.8920*	0.1380	2142.06	0.11
		+ watertempmean	-0.0162*	0.0080					
	~1	~pool_depth_mean	-0.0043	0.0075	~pool_depth_mean	0.8570*	0.1530	2142.15	0.11
		+ watertempmean	-0.0162*	0.0080					
	~1	~watertempmean	-0.0140	0.0131	~pool_depth_mean	0.8570*	0.1440	2142.48	0.09
		+ day	-0.0001	0.0005					
BI	~1	~pool_depth_mean	0.0128*	0.0046	~pool_depth_mean	0.2902*	0.1222	2824.74	0.30
		+ watertempmean	-0.0103	0.0092	+ rain24	0.0563	0.0474		
		+ day	-0.0015*	0.0004	+ day	0.0411*	0.0096		
	~1	~pool_depth_mean	0.0097*	0.0042	~pool_depth_mean	0.3085*	0.1151	2824.85	0.28
		+ day	-0.0017*	0.0003	+ rain24	0.0500	0.0333		
					+ day	0.0146	0.0147		
	~1	~pool_depth_mean	0.0130*	0.0044	~pool_depth_mean	0.1983	0.1054	2826.00	0.16
		+ rain7	0.0133	0.0073	+ rain24	0.1051	0.0694		
		+ day	-0.0021*	0.0004	+ day	0.0453*	0.0068		
		+ pool_depth_mean : rain7	-0.0038	0.0050					
	~1	~pool_depth_mean	0.0140*	0.0044	~pool_depth_mean	0.2052*	0.1047	2826.74	0.11
		+ watertempmean	-0.0057	0.0100	+ rain24	0.1017	0.0633		
		+ day	-0.0019*	0.0004	+ day	0.0452*	0.0070		
		+ rain7	0.0103	0.0077					
TA	~1	~watertempmean	-0.0128*	0.0043	~pool_depth_mean	0.5406*	0.1291	3461.54	0.39
					+ rain24	-0.0154	0.0309		
					+ day	-0.0240*	0.0041		
	~1	~pool_depth_mean	0.0029	0.0037	~pool_depth_mean	0.5119*	0.1392	3462.88	0.20
		+ watertempmean	-0.0124*	0.0043	+ rain24	-0.0181	0.0313		
					+ day	-0.0244*	0.0042		
	~1	~rain7	-0.0030	0.0049	~pool_depth_mean	0.5367*	0.1305	3463.20	0.17
		+ watertempmean	-0.0141*	0.0049	+ rain24	-0.0241	0.0339		
					+ day	-0.0234*	0.0044		

Note: All streams were fitted with the 'pcountopen' function from the 'unmarked' package (Fiske & Chandler, 2011) with the following setting: dynamics = "trend", immigration = "T" and mixture = "NB". Initial abundance was not affected by any covariate in all models, as shown by ~1, that refers to a constant parameter. The models listed in this table have shown an AIC value of ≤ 2 compared to the highest ranking model. Pool_depth_mean, rain7, rain24 and watertempmean have been standardized prior to the analysis to a mean of zero and a standard deviation of one. Asterisks indicate the statistical significance ($\alpha = 0.05$), while ':' stands for interaction. The following abbreviations were used for the streams: DI = Diegterbach, CH = Chrintelbach, BI = Binzholdengraben, TA = Talbächli. Further abbreviations, as well as their descriptions, are listed in Table 2.

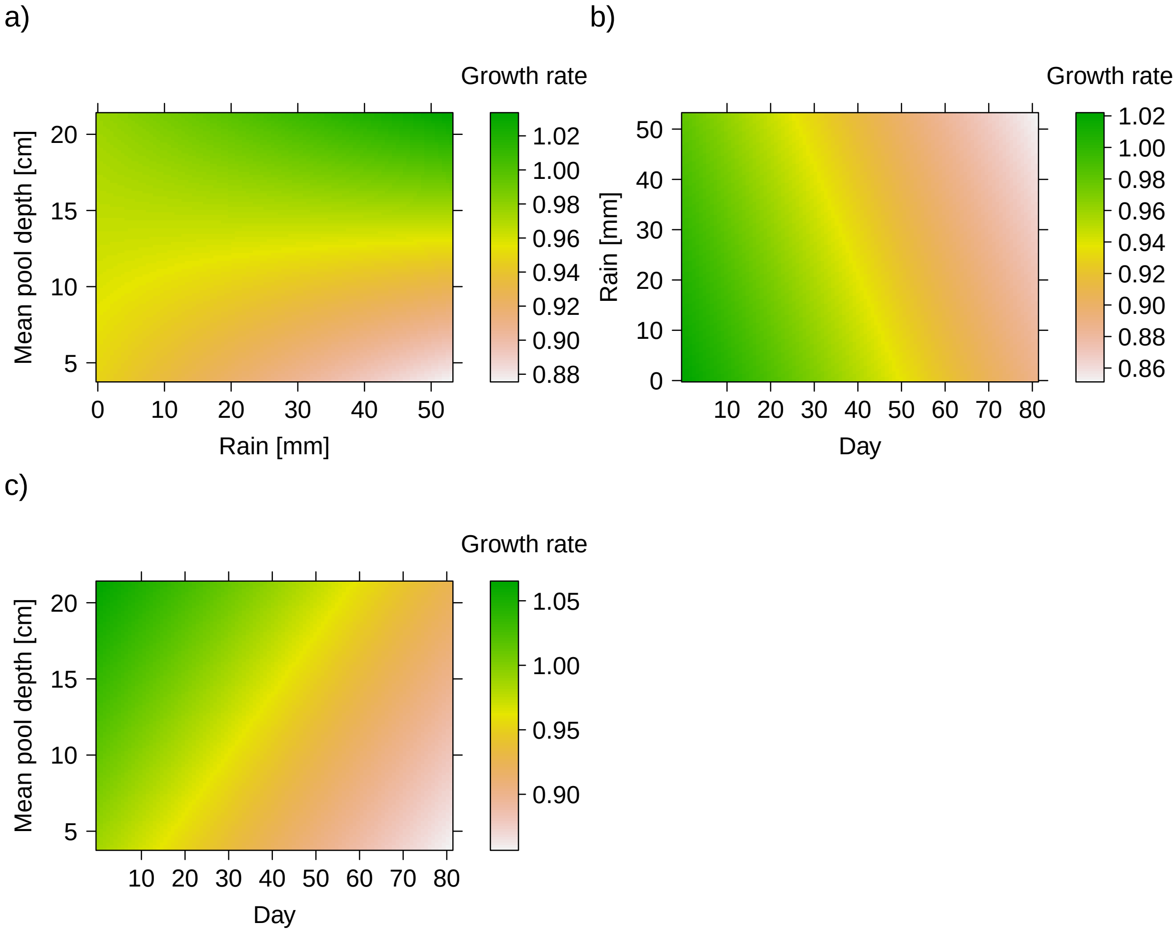

Figure 4: Predicted growth rate dependent on a) rain and mean pool depth, b) day and rain and c) day and mean pool depth in Diegterbach.

Figure 4 shows the relationship between growth rate and the variables mean pool depth, rain and day. Interestingly, growth rate was found to be highest with large pool depths and high rainfall, whereas it was lowest with small pool depths and high rainfall (Figure 4 a)). An interaction term was found to be positively significant in Diegterbach (Table 3). The lower growth rates could have been caused by rain having a higher flush out effect on larvae inhabiting lower pool depths, leading them to drift much faster than larvae inhabiting deeper pools. Additionally, rain later in the season was affecting growth rate more drastically than the same amount of rainfall earlier in the season (Figure 4 b)). Pool depth had a positive influence on growth rate over the whole study period, while growth rate is decreasing with an increasing amount of days (Figure 4 c). Concluding, growth rate was highest for a population inhabiting a deep pool, early in the season with low rainfall, whereas in the deepest pools (20 cm pool depth) high rainfall was positively influencing growth rate. (Figure 4 b) and c)).

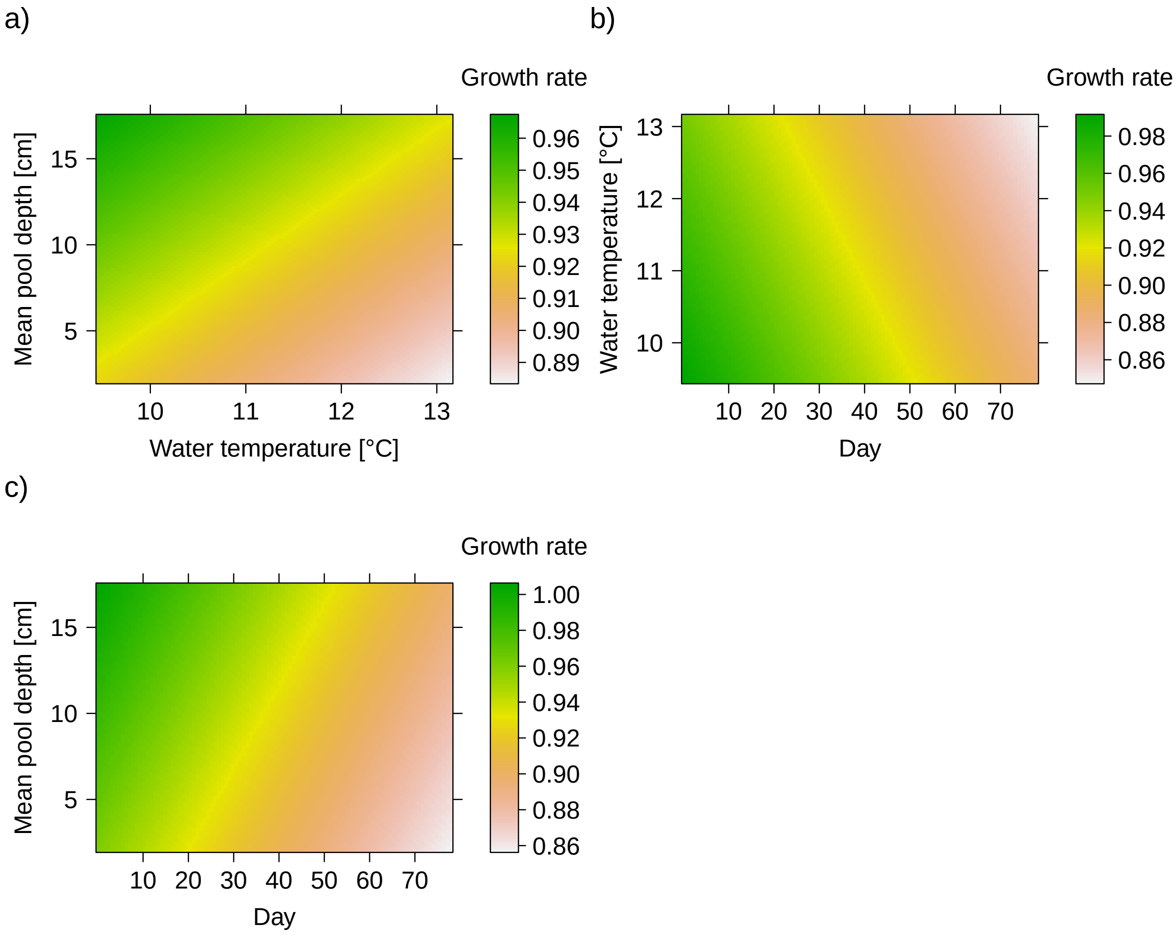

Figure 5: Predicted growth rate dependent on a) water temperature and mean pool depth, b) day and rain and c) day and mean pool depth in stream Binzholdengraben.

A large pool depth combined with a low water temperature showed the highest growth rate in stream Binzholdengraben, whereas a small pool depth and a high water temperature led to a lower growth rate (Figure 5 a)). A higher water temperature later in the season had a larger impact on a population's growth rate than the same temperature had earlier in the season (Figure 5 b)). Additionally, the same effects were identified here: A larval population inhabiting a deep pool at the beginning of the season represented a higher growth rate (Figure 5 c)). This could be explained by deeper pools warming up slower, as well as naturally occurring lower above ground temperatures earlier in the season, both leading to a lower water temperature.

Overall, the growth rate of a larval population is highest when their pool depth is large, it is early in the season, the amount of rain fallen is low and the water temperature is low.

4 Discussion

Understanding factors underlying population abundance and their growth rates are important for a better understanding of the larval stage of the fire salamander and to determine effective conservation strategies. I found larvae to be more abundant in deeper pools, indicating that this may be the habitat feature which is most important in determining stream quality for salamander larvae. Furthermore, increasing water temperatures, later date in the season, as well as a higher amount of rain were associated with a lower population growth rate, suggesting a negative impact on larval survival.

4.1 Detection probability

In this study, detection probability was found to be positively affected by larger pool depths. This could be due to a preference of females to deposit their larvae into deeper and larger pools (Segev et al., 2011). Thus, deeper pools accommodate a larger number of larvae, which leads to a higher density and a consequent higher visibility thereof. Although, all streams showed a significant impact of pool depth on detection probability, the detection probability increased in two, whereas it decreased in one stream with the ongoing study duration (Table 3). The increasing detection probability over time may be explained by the experience I collected over time and/or larger larval body sizes of later stages (also found by Wagner, Harms, et al. (2020)). In the one stream (Table 3; TA), where detection probability decreased, one process that might have played a role is larval drift, as suggested by Wagner, Lötters, et al. (2020).

4.2 Larval abundance , initial abundance and growth rate

4.2.1 Larval abundance pattern

The overall deposition of larvae exhibited a peak in early May (i.e., week four; Figure 3), which has probably been caused by a dry period from mid-March to the end of April. This is in agreement with Thiesmeier (1992) and Schlüpmann & Kupfer (2009) findings that larvae are being deposited between early March and mid-May, varying with suitable climatic conditions (e.g., spring rains). Furthermore, the less larvae found during the dry period are consistent with the finding that females are capable of delaying larval deposition depending on the weather (Segev et al., 2011), an ability which helps females to ensure larval survival under stressful conditions (e.g., drought). Generally, over the whole study period, the temporal dynamics between streams were different but underlie all a certain seasonal effect (i.e., increase in abundance at the beginning of the season, this might even be before observations for this study started, and a consequent decrease in abundance after metamorphosis). The later in the season, the lower were the larval abundance estimates. Mortality has been shown to depend for example on predation pressure (Petranka, 1983) or pool desiccation (Wilbur, 1980). In this study, there were no predators present in any of the four streams, what could be due to their small size and therefore predation as a cause of mortality can be excluded. Pool desiccation often occurs to a preceding termination of freshwater income and a subsequent deterioration in water quality. Low water quality can in extreme cases lead to the extinction of a population, which was observed in this study especially in Chrintelbach. In this study, the decline in abundance was taken as a proxy for mortality since larvae are bound to an aquatic habitat until metamorphosis.

4.2.2 Model estimations: Initial abundance and growth rate

The best model differed between streams, while in two best models pool depth affected growth rate positively (Table 3; DI, BI), water temperature had a negative impact on growth rate in three models (Table 3; CH, BI, TA) and rain had shown a negative effect in only one stream (Table 3; DI). This suggests that the dynamic of a larval population is not influenced by the same environmental factors in each stream. Initial abundance was not affected by pool depth, revealing the same initial number of larvae in each pool per stream. Nevertheless, while modelling the initial abundance part, in each stream the second-best model was with the covariate pool depth and therefore, an influence cannot be excluded. Furthermore, larger pool depths positively affected the population growth rate. This is in agreement with a study carried out by Hannappel & Schiefenhövel (2013), where pool depth had a positive effect on larval presence in a stream. Several studies have outlined the positive influence of an increasing number of pools in a stream on larval abundance (Baumgartner et al., 1999; Schmidt et al., 2015; Wagner, Harms, et al., 2020). With an increasing number of pools, the probability that some of them are deeper gets higher. Therefore, the knowledge of the importance of pool depth on larval presence and number of pools on larval abundance can be expanded to pool depth having an influence on a population's growth rate. Thus, modifications (e.g., straightening of a stream or a streambed) of a stream, which serves as a natural habitat to fire salamander larvae, potentially affect population growth rates negatively. The upper boundary of the pool depth was not identified in this study, but is thought to be around 20 cm (Manenti et al., 2009) because larger pool depths are often related to fish presence and hence a higher predation pressure (Hannappel & Schiefenhövel, 2013). Lastly, a significant interaction between mean pool depth and rain was found to positively influence growth rate in Diegterbach (Table 3; DI); and highest growth rates were predicted for a high amount of rain and a large pool depth. This indicates on an importance of larger pool depths causing less flush-out events of larvae. Previous studies concerning larval drift have shown that heavy rainfalls increase the water velocity and result in an extreme reduction of larvae, where especially smaller larvae are affected (Thiesmeier & Schuhmacher, 1990). Henceforth, larger pools could serve as a buffer for inhabiting larvae as well as a catch basin for from upstream drifting larvae. Nevertheless, whether rain has an impact on growth rate is also dependent on the stream's structure (e.g., riffles or number of pools which serve as hiding places for larvae). A stream with smaller pool depths and low heterogeneity is therefore thought to be more sensitive on heavy rainfall than a stream with larger pool depths and high heterogeneity. Warmer temperatures generally increase the development time in ectotherms (Berrigan & Charnov, 1994). Conversely, in this study, water temperature affected the growth rate of larval populations negatively (Table 3). One process underlying this effect could consist of warmer temperatures leading to a shrinkage of pool sizes and thus a higher probability of a pool to dry out accompanied by a higher extinction risk of a population. Therefore, streamside forests are of high importance, as they have been shown to serve as a buffer for increasing temperatures (Sweeney & Newbold, 2014). Forest cover does not only directly impact the adult fire salamander's abundance, but through this also indirectly the larval abundance (Hannappel & Schiefenhövel, 2013; Manenti et al., 2009). When forest cover near a stream inhabited by larvae is reduced (i.e., by deforestation), the natural buffer system "forest" gets removed. The stream becomes unprotected against extreme temperatures and temperature fluctuations are likely to become more common. Moreover, with higher temperatures, evaporation rates of the water are also increasing and lead to shallower water levels (Corn & Muths, 2002), which again lead to more variable temperatures and a faster water loss. Furthermore, deforestation has been shown to negatively affect adults as well (Schmidt et al., 2005). Thus, a deeper pool could again be a potential advantage with increasing temperatures because warming up proceeds slower.

This work has outlined several environmental factors that influence the abundance patterns and growth rates in larval fire salamander populations. In conclusion, the environmental factors influencing population growth rate differed between streams. Furthermore, this study indicated that increasing water temperatures negatively affect a populations' growth rate. With the ongoing climate change, temperature is increasing and so do water temperatures of streams (Blaustein et al., 2010). Therefore, this could be of particular interest also for further research. Furthermore, deeper pools led to a faster growth rate, assumed to be due to lower flush out effects of larvae and a slower warming of the pools. Amphibian populations have been reported to undergo strong fluctuations in their sizes on a yearly scale (Schmidt, 2018; Semlitsch, 2000). With long-term studies of larval salamanders, these observed growth rates can be better assessed and compared. This study could help decision makers, as it highlights environmental factors that affect the development of a larval population. Management strategies such as a regulation of deforestation near habitats of the fire salamander and stream preservation in their natural flow (and especially pool depth) are of high importance.

Acknowledgements

I would like to thank Dr. Benedikt Schmidt and Prof. Dr. Arpat Ozgul for their supervision and support during this study. It has been a though year, marked by the COVID-19 pandemic and this project has been in jeopardy. Nevertheless, they were always available throughout this year, supported me greatly with their help and made it possible to carry on with this project. I thank the whole popecol group for their help and discussions, when problems arose during the study. Furthermore, I want to thank Dr. Simon Aeschbacher and Dr. Ursina Tobler for their valuable lectures in a scientific writing course, as well as Benedetta Catitti, Nico Santavenere and Anna Glaus for proof reading my master thesis. Lastly, I want to thank my family for their motivation, as well as their financial and mental support.

Statement of Authorship

I declare that I have used no other sources and aids other than those indicated. All passages quoted from publications or paraphrased from these sources are indicated as such, i.e. cited and/or attributed. This thesis was not submitted in any form for another degree or diploma at any university or other institution of tertiary education.

Zurich, Date
Signature

References

Baumgartner, N., Waringer, A., & Waringer, J. (1999). Hydraulic microdistribution patterns of larval fire salamanders (Salamandra salamandra salamandra) in the Weidlingbach near Vienna , Austria. *Freshwater Biology*, *41*, 31–41.

Beebee, T. J. (1995). Amphibian breeding and climate. *Nature*, *374*(6519), 219–220. doi: 10.1038/374219a0

Beebee, T. J., Denton, J. S., & Buckley, J. (1996). Factors affecting population densities of adult natterjack toads Bufo calamita in Britain. *British Ecological Society*, *33*(2), 263–268. doi: 10.2307/2404748

Benton, T. G., & Grant, A. (1999). Elasticity analysis as an important tool in evolutionary and population ecology. *Trends in Ecology and Evolution*, *14*(12), 467–471. doi: 10.1016/S0169-5347(99)01724-3

Berrigan, D., & Charnov, E. L. (1994). Reaction Norms for Age and Size at Maturity in Response to Temperature: A Puzzle for Life Historians. *Oikos*, *70*(3), 474–478. doi: 10.2307/3545787

Biek, R., Funk, W. C., Maxell, B. A., & Mills, L. S. (2002). What is missing in amphibian decline research: Insights from ecological sensitivity analysis. *Conservation Biology*, *16*(3), 728–734. doi: 10.1046/j.1523-1739.2002.00433.x

Blaustein, A. R., & Kiesecker, J. M. (2002). Complexity in conservation: Lessons from the global decline of amphibian populations. *Ecology Letters*, *5*(4), 597–608. doi: 10.1046/j.1461-0248.2002.00352.x

Blaustein, A. R., Walls, S. C., Bancroft, B. A., Lawler, J. J., Searle, C. L., & Gervasi, S. S. (2010). Direct and indirect effects of climate change on amphibian populations. *Diversity*, *2*(2), 281–313. doi: 10.3390/d2020281

Cayuela, H., Olgun, K., Angelini, C., Üzüm, N., Peyronel, O., Miaud, C., ... Schmidt, B. R. (2019, aug). Slow life-history strategies are associated with negligible actuarial senescence in western Palaearctic salamanders. *Proceedings of the Royal Society B: Biological Sciences*, *286*(1909). doi: 10.1098/rspb.2019.1498

Corn, P. S., & Muths, E. (2002). Variable breeding phenology affects the exposue of amphibian embryos to ultraviolet radiation. *Ecology*, *83*(11), 2958–2963.

Dail, D., & Madsen, L. (2011). Models for Estimating Abundance from Repeated Counts of an Open Metapopulation. *Biometrics*, *67*(2), 577–587. doi: 10.1111/j.1541-0420.2010.01465.x

Dorcas, M. E., Willson, J. D., & Gibbons, J. W. (2007). Crab trapping causes population decline and demographic changes in diamondback terrapins over two decades. *Biological Conservation*, *137*(3), 334–340. doi: 10.1016/j.biocon.2007.02.014

Duellman, W. E., & Trueb, L. (1994). *Biology of Amphibians.* doi: 10.1086/418798

Fiske, I. J., & Chandler, R. B. (2011). unmarked: An R Package for Fitting Hierarchical Models of Wildlife Occurrence and Abundance. *Journal of Statistical Software*, *43*(10).

GoogleMaps. (2020). *Map of Sissach.* Retrieved 2020-07-24, from `https://www.google.ch/maps/place/4450+Sissach/@47.46864,7.7911304,13.44z/data=!4m5!3m4!1s0x47903527c5c23b4b:0x7239c03e423d21ba!8m2!3d47.4643945!4d7.810661`

Govindarajulu, P. P., & Anholt, B. R. (2006). Interaction between biotic and abiotic factors determines tadpole survival rate under natural conditions. *Ecoscience*, *13*(3), 413–421.

Hannappel, A., & Schiefenhövel, P. (2013). Populationsökologische Untersuchung zum Feuersalamander (Salamandra salamandra) in zwei FFH-Gebieten auf der Montabaurer Höhe, Westerwaldkreis, Rheinland-Pfalz. *Will und Liselott Masgeik-Stiftung für Natur- und Landschaftsschutz*, *11*.

Hoffmann, M., Hilton-Taylor, C., Angulo, A., Böhm, M., Brooks, T. M., Butchart, S. H., … Stuart, S. N. (2010, dec). The impact of conservation on the status of the world's vertebrates. *Science*, *330*(6010), 1503–1509. doi: 10.1126/science.1194442

Hostetler, J. A., & Chandler, R. B. (2015). Improved state-space models for inference about spatial and temporal variation in abundance from count data. *Ecology*, *96*(6), 1713–1723. doi: 10.1890/14-1487.1

Jones, M. T., Milligan, W. R., Kats, L. B., Vandergon, T. L., Honeycutt, R. L., Fisher, R. N., … Lucas, T. A. (2017). A discrete stage-structured model of California newt population dynamics during a period of drought. *Journal of Theoretical Biology*, *414*, 245–253. doi: 10.1016/j.jtbi.2016.11.011

Kéry, M., & Royle, J. A. (2016). *Applied Hierarchical Modeling in Ecology - Analysis of distribution, abundance and species richness in R and BUGS* (Vol. 1). Elsevier Inc.

Kéry, M., & Royle, J. A. (2020). *Applied Hierarchical Modeling in Ecology.* Elsevier Inc. doi: 10.1016/c2013-0-19160-x

Manenti, R., Ficetola, G. F., & De Bernardi, F. (2009). Water, stream morphology and landscape: complex habitat determinants for the fire salamander Salamandra salamandra. *Amphibia-Reptilia*, *30*, 7–15.

MeteoSwiss. (2020). *Weather data from Sissach.* Retrieved 2020-08-05, from `https://www.meteoswiss.admin.ch/home/measurement-values.html?param=messwerte-niederschlag-1d&station=RUE&chart=day`

Pechmann, J. H., & Wilbur, H. M. (1994). Putting declining amphibian populations in perspective: Natural fluctuations and human impacts. *Herpetologica*, *50*(1), 65–84.

Petranka, J. W. (1983). Fish Predation: A Factor Affecting the Spatial Distribution of a Stream-Breeding Salamander. *Copeia*, *1983*(3), 624–628.

Petrovan, S. O., & Schmidt, B. R. (2016). Volunteer conservation action data reveals large-scale and long-term negative population trends of a widespread amphibian, the common toad (Bufo bufo). *PLoS ONE*, *11*(10), 12. doi: 10.1371/journal.pone.0161943

Petrovan, S. O., & Schmidt, B. R. (2019). Neglected juveniles; a call for integrating all amphibian life stages in assessments of mitigation success (and how to do it). *Biological Conservation*, *236*, 252–260. doi: 10.1016/j.biocon.2019.05.023

R Core Team. (2020). *R: A Language and Environment for Statistical Computing.* Vienna, Austria. Retrieved from `https://www.r-project.org/`

Sandvoß, M., Wagner, N., Lötters, S., Feldmeier, S., Schulz, V., Steinfartz, S., & Veith, M. (2020). Spread of the pathogen batrachochytrium salamandrivorans and large-scale absence of larvae suggest unnoticed declines of the European fire salamander in the southern eifel mountains. *Salamandra*, *56*(3), 215–226.

Schindelin, J., Arganda-Carreras, I., Frise, E., Kaynig, V., Longair, M., Pietzsch, T., … Cardona, A. (2012). Fiji: An open-source platform for biological-image analysis. *Nature Methods*, *9*(7), 676–682. doi: 10.1038/nmeth.2019

Schlüpmann, M., & Kupfer, A. (2009). Methoden der Amphibienerfassung – eine Übersicht. *Zeitschrift für Feldherpetologie*, 7–84.

Schmidt, B. R. (2011). Die Bedeutung der Jungtiere für die Populationsdynamik von Amphibien. *Zeitschrift fur Feldherpetologie*, *18*(2), 129–136.

Schmidt, B. R. (2018). Wie funktionieren Amphibien-Populationen? *Zeitschrift für Feldherpetologie*, *25*, 166–183.

Schmidt, B. R., Feldmann, R., & Schaub, M. (2005). Demographic processes underlying population growth and decline in Salamandra salamandra. *Conservation Biology*, *19*(4), 1149–1156. doi: 10.1111/j.1523-1739.2005.00164.x

Schmidt, B. R., Gschwend, G., Bachmann, J. A., & Dermond, P. (2015). Use of removal sampling to estimate abundance of larval salamanders (Salamandra salamandra) in streams. *Amphibia Reptilia*, *36*(1), 87–92. doi: 10.1163/15685381-00002981

Schmidt, B. R., & Zumbach, S. (2005). Rote Liste der gefährdeten Arten der Schweiz: Amphibien. (Vollzug Umwelt VU).

Segev, O., & Blaustein, L. (2014). Influence of water velocity and predation risk on fire salamander (Salamandra infraimmaculata) larval drift among temporary pools in ephemeral streams. *Freshwater Science*, *33*(3), 950–957. doi: 10.1086/676634

Segev, O., Mangel, M., Wolf, N., Sadeh, A., Kershenbaum, A., & Blaustein, L. (2011). Spatiotemporal reproductive strategies in the fire salamander: A model and empirical test. *Behavioral Ecology*, *22*(3), 670–678. doi: 10.1093/beheco/arr029

Semlitsch, R. D. (2000). Principles for Management of Aquatic-Breeding Amphibians. *Wildlife Society*, *64*(3), 615–631. doi: 10.2307/3802732

Strahler, A. N. (1957). Quantitative Analysis of Watershed Geomorphology. *Eos, Transactions of the American Geophysical Union.* doi: 10.1029/TR038i006p00913

Stuart, S. N., Chanson, J. S., Cox, N. A., Young, B. E., Rodrigues, A. S., Fischman, D. L., & Waller, R. W. (2004). Status and trends of amphibian declines and extinctions worldwide. *Science*, *306*(5702), 1783–1786. doi: 10.1126/science.1103538

Sweeney, B. W., & Newbold, J. D. (2014). Streamside forest buffer width needed to protect stream water quality, habitat, and organisms: A literature review. *Journal of the American Water Resources Association*, *50*(3), 560–584. doi: 10.1111/jawr.12203

Thiesmeier, B. (1992). *Ökologie des Feuersalamanders.* Westarp Wiss.

Thiesmeier, B., & Schuhmacher, H. (1990). Causes of larval drift of the fire salamander, Salamandra salamandra terrestris, and its effects on population dynamics. *Oecologia*, *82*(2), 259–263. doi: 10.1007/BF00323543

Wagner, N., Harms, W., Hildebrandt, F., Martens, A., Ong, S. L., Wallrich, K., … Veith, M. (2020). Do habitat preferences of european fire salamander (Salamandra salamandra) larvae differ among landscapes? A case study from Western Germany. *Salamandra*, *56*(3), 254–264.

Wagner, N., Lötters, S., Dalbeck, L., Düssel, H., Guschal, M., Kirst, K., … Veith, M. (2020). Long-term monitoring of European fire salamander populations (Salamandra salamandra) in the Eifel Mountains (Germany): five years of removal sampling of larvae. *Salamandra, 56*(3), 243–253.

Wagner, N., Pfrommer, J., & Veith, M. (2020). Comparison of different methods to estimate abundances of larval fire salamanders (Salamandra salamandra) in first-order creeks. *Salamandra, 56*(3), 265–274.

Wilbur, H. M. (1980, nov). Complex Life Cycles. *Annual Review of Ecology and Systematics, 11*(1), 67–93. doi: 10.1146/annurev.es.11.110180.000435

5 Appendix

Table 4: Model selection for Diegterbach. All 26 candidate models of each stream are displayed with their respective AIC-value, difference in AIC to the best model (Δ), AIC-weight (AICwt) and cumulative AIC-weight (cumltvWt).

Initial Abundance	Growth rate	Detection probability	AIC	Δ	AICwt	cumltvWt
~1	~1	~pool_depth_mean + day	3199.650	0.0000	0.5732	0.5732
~1	~1	~pool_depth_mean + rain24 + day	3200.261	0.6111	0.4223	0.9954
~1	~1	~day	3210.128	10.4780	0.0030	0.9985
~1	~1	~rain24 + day	3211.501	11.8504	0.0015	1.0000
~1	~1	~1	3233.208	33.5577	0.0000	1.0000
~1	~1	~rain24	3234.962	35.3115	0.0000	1.0000
~1	~1	~pool_depth_mean	3234.965	35.3146	0.0000	1.0000
~1	~1	~pool_depth_mean + rain24	3236.662	37.0121	0.0000	1.0000
~1	~1	~pool_depth_mean + day	3199.650	0.0000	0.7311	0.7311
~pool_depth_mean	~1	~pool_depth_mean + day	3201.650	2.0000	0.2689	1.0000
~1	~1	~1	3233.208	33.5577	0.0000	1.0000
~1	~pool_depth_mean * rain7 + day	~pool_depth_mean + day	3167.136	0.0000	0.7221	0.7221
~1	~pool_depth_mean + rain7 + watertempmean + day	~pool_depth_mean + day	3169.982	2.8455	0.1740	0.8961
~1	~pool_depth_mean + rain7 + day	~pool_depth_mean + day	3171.370	4.2333	0.0870	0.9831
~1	~pool_depth_mean + day	~pool_depth_mean + day	3176.192	9.0555	0.0078	0.9909
~1	~pool_depth_mean + watertempmean + day	~pool_depth_mean + day	3177.353	10.2161	0.0044	0.9952
~1	~pool_depth_mean * rain7 + watertempmean	~pool_depth_mean + day	3177.485	10.3486	0.0041	0.9993
~1	~pool_depth_mean * rain7	~pool_depth_mean + day	3181.770	14.6339	0.0005	0.9998
~1	~rain7 + watertempmean + day	~pool_depth_mean + day	3184.006	16.8690	0.0002	1.0000
~1	~rain7 + watertempmean	~pool_depth_mean + day	3188.170	21.0336	0.0000	1.0000
~1	~pool_depth_mean + rain7 + watertempmean	~pool_depth_mean + day	3188.403	21.2666	0.0000	1.0000
~1	~pool_depth_mean + rain7	~pool_depth_mean + day	3190.586	23.4494	0.0000	1.0000
~1	~watertempmean + day	~pool_depth_mean + day	3193.525	26.3883	0.0000	1.0000
~1	~pool_depth_mean + watertempmean	~pool_depth_mean + day	3198.880	31.7435	0.0000	1.0000
~1	~watertempmean	~pool_depth_mean + day	3199.086	31.9492	0.0000	1.0000
~1	~pool_depth_mean	~pool_depth_mean + day	3199.086	31.9492	0.0000	1.0000
~1	~1	~pool_depth_mean + day	3233.208	66.0715	0.0000	1.0000
~1	~day	~pool_depth_mean + day	41102.992	37935.8558	0.0000	1.0000
~1	~rain7	~pool_depth_mean + day	41102.992	37935.8558	0.0000	1.0000
~1	~rain7 + day	~pool_depth_mean + day	41102.992	37935.8558	0.0000	1.0000

Table 5: Model selection for Chrintelbach. All 26 candidate models of each stream are displayed with their respective AIC-value, difference in AIC to the best model (Δ), AIC-weight (AICwt) and cumulative AIC-weight (cumltvWt).

Initial Abundance	Growth rate	Detection probability	AIC	Δ	AICwt	cumltvWt
~1	~1	~pool_depth_mean	2142.679	0.0000	0.4896	0.4896
~1	~1	~pool_depth_mean + day	2144.164	1.4850	0.2330	0.7226
~1	~1	~pool_depth_mean + rain24	2144.571	1.8919	0.1901	0.9127
~1	~1	~pool_depth_mean + rain24 + day	2146.128	3.4488	0.0873	1.0000
~1	~1	~day	2166.498	23.8195	0.0000	1.0000
~1	~1	~1	2168.054	25.3752	0.0000	1.0000
~1	~1	~rain24 + day	2168.393	25.7144	0.0000	1.0000
~1	~1	~rain24	2170.049	27.3701	0.0000	1.0000
~1	~1	~pool_depth_mean	2142.679	0.0000	0.6295	0.6295
~pool_depth_mean	~1	~pool_depth_mean	2143.739	1.0600	0.3705	1.0000
~1	~1	~1	2168.054	25.3752	0.0000	1.0000
~1	~watertempmean	~pool_depth_mean	2140.478	0.0000	0.2481	0.2481
~1	~rain7 + watertempmean	~pool_depth_mean	2142.061	1.5835	0.1124	0.3606
~1	~pool_depth_mean + watertempmean	~pool_depth_mean	2142.153	1.6755	0.1074	0.4679
~1	~watertempmean + day	~pool_depth_mean	2142.478	2.0000	0.0913	0.5592
~1	~day	~pool_depth_mean	2142.687	2.2090	0.0822	0.6414
~1	~rain7 + watertempmean + day	~pool_depth_mean	2142.859	2.3811	0.0754	0.7169
~1	~pool_depth_mean + rain7 + watertempmean	~pool_depth_mean	2143.758	3.2802	0.0481	0.7650
~1	~pool_depth_mean + watertempmean + day	~pool_depth_mean	2144.153	3.6755	0.0395	0.8045
~1	~pool_depth_mean	~pool_depth_mean	2144.381	3.9026	0.0353	0.8398
~1	~rain7	~pool_depth_mean	2144.424	3.9462	0.0345	0.8743
~1	~pool_depth_mean + day	~pool_depth_mean	2144.531	4.0526	0.0327	0.9070
~1	~pool_depth_mean + rain7 + watertempmean + day	~pool_depth_mean	2144.663	4.1851	0.0306	0.9376
~1	~rain7 + day	~pool_depth_mean	2144.700	4.2223	0.0300	0.9676
~1	~pool_depth_mean + rain7	~pool_depth_mean	2146.138	5.6604	0.0146	0.9823
~1	~pool_depth_mean + rain7 + day	~pool_depth_mean	2146.505	6.0269	0.0122	0.9945
~1	~pool_depth_mean * rain7	~pool_depth_mean	2148.082	7.6041	0.0055	1.0000
~1	~1	~pool_depth_mean	2168.054	27.5761	0.0000	1.0000
~1	~pool_depth_mean * rain7 + day	~pool_depth_mean	2707.336	566.8579	0.0000	1.0000
~1	~pool_depth_mean * rain7 + watertempmean	~pool_depth_mean	2760.056	619.5778	0.0000	1.0000

Table 6: Model selection for stream Binzholdengraben. All 26 candidate models of each stream are displayed with their respective AIC-value, difference in AIC to the best model (Δ), AIC-weight (AICwt) and cumulative AIC-weight (cumltvWt).

Initial Abundance	Growth rate	Detection probability	AIC	Δ	AICwt	cumltvWt
~1	~1	~pool_depth_mean + rain24 + day	2831.212	0.0000	0.8243	0.8243
~1	~1	~pool_depth_mean + day	2834.316	3.1033	0.1747	0.9989
~1	~1	~rain24 + day	2845.166	13.9536	0.0008	0.9997
~1	~1	~day	2847.100	15.8873	0.0003	1.0000
~1	~1	~pool_depth_mean + rain24	2862.860	31.6478	0.0000	1.0000
~1	~1	~pool_depth_mean	2864.125	32.9126	0.0000	1.0000
~1	~1	~rain24	2871.672	40.4594	0.0000	1.0000
~1	~1	~1	2872.509	41.2964	0.0000	1.0000
~1	~1	~pool_depth_mean + rain24 + day	2831.212	0.0000	0.7244	0.7244
~pool_depth_mean	~1	~pool_depth_mean + rain24 + day	2833.145	1.9323	0.2756	1.0000
~1	~1	~1	2872.509	41.2964	0.0000	1.0000
~1	~pool_depth_mean + watertempmean + day	~pool_depth_mean + rain24 + day	2824.740	0.0000	0.2962	0.2962
~1	~pool_depth_mean + day	~pool_depth_mean + rain24 + day	2824.851	0.1115	0.2802	0.5764
~1	~pool_depth_mean * rain7 + day	~pool_depth_mean + rain24 + day	2825.998	1.2587	0.1579	0.7343
~1	~pool_depth_mean + rain7 + watertempmean + day	~pool_depth_mean + rain24 + day	2826.740	2.0000	0.1090	0.8433
~1	~pool_depth_mean + rain7 + day	~pool_depth_mean + rain24 + day	2826.851	2.1115	0.1031	0.9463
~1	~day	~pool_depth_mean + rain24 + day	2830.995	6.2559	0.0130	0.9593
~1	~pool_depth_mean	~pool_depth_mean + rain24 + day	2832.470	7.7309	0.0062	0.9655
~1	~watertempmean	~pool_depth_mean + rain24 + day	2832.494	7.7541	0.0061	0.9716
~1	~rain7 + day	~pool_depth_mean + rain24 + day	2832.865	8.1259	0.0051	0.9767
~1	~watertempmean + day	~pool_depth_mean + rain24 + day	2832.913	8.1735	0.0050	0.9817
~1	~rain7	~pool_depth_mean + rain24 + day	2833.200	8.4600	0.0043	0.9860
~1	~pool_depth_mean + watertempmean	~pool_depth_mean + rain24 + day	2833.341	8.6019	0.0040	0.9900
~1	~rain7 + watertempmean	~pool_depth_mean + rain24 + day	2834.365	9.6250	0.0024	0.9924
~1	~pool_depth_mean + rain7	~pool_depth_mean + rain24 + day	2834.463	9.7236	0.0023	0.9947
~1	~rain7 + watertempmean + day	~pool_depth_mean + rain24 + day	2834.658	9.9180	0.0021	0.9968
~1	~pool_depth_mean + rain7 + watertempmean	~pool_depth_mean + rain24 + day	2835.156	10.4160	0.0016	0.9984
~1	~pool_depth_mean * rain7	~pool_depth_mean + rain24 + day	2836.369	11.6290	0.0009	0.9993
~1	~pool_depth_mean * rain7 + watertempmean	~pool_depth_mean + rain24 + day	2836.911	12.1718	0.0007	1.0000
~1	~1	~pool_depth_mean + rain24 + day	2872.509	47.7692	0.0000	1.0000

Table 7: Model selection for Talbächli. All 26 candidate models of each stream are displayed with their respective AIC-value, difference in AIC to the best model (Δ), AIC-weight (AICwt) and cumulative AIC-weight (cumltvWt).

Initial Abundance	Growth rate	Detection probability	AIC	Δ	AICwt	cumltvWt
~1	~1	~pool_depth_mean + rain24 + day	3468.519	0.0000	0.6998	0.6998
~1	~1	~pool_depth_mean + day	3470.241	1.7222	0.2958	0.9955
~1	~1	~rain24 + day	3478.853	10.3339	0.0040	0.9995
~1	~1	~day	3483.163	14.6434	0.0005	1.0000
~1	~1	~pool_depth_mean	3492.722	24.2023	0.0000	1.0000
~1	~1	~pool_depth_mean + rain24	3493.823	25.3035	0.0000	1.0000
~1	~1	~rain24	3495.706	27.1870	0.0000	1.0000
~1	~1	~1	3495.759	27.2396	0.0000	1.0000
~1	~1	~pool_depth_mean + rain24 + day	3468.519	0.0000	0.7311	0.7311
~pool_depth_mean	~1	~pool_depth_mean + rain24 + day	3470.519	2.0000	0.2689	1.0000
~1	~1	~1	3495.759	27.2396	0.0000	1.0000
~1	~watertempmean	~pool_depth_mean + rain24 + day	3461.544	0.0000	0.3925	0.3925
~1	~pool_depth_mean + watertempmean	~pool_depth_mean + rain24 + day	3462.882	1.3385	0.2010	0.5934
~1	~rain7 + watertempmean	~pool_depth_mean + rain24 + day	3463.195	1.6517	0.1719	0.7653
~1	~pool_depth_mean + rain7 + watertempmean	~pool_depth_mean + rain24 + day	3464.570	3.0262	0.0864	0.8517
~1	~rain7 + watertempmean + day	~pool_depth_mean + rain24 + day	3465.195	3.6517	0.0632	0.9149
~1	~pool_depth_mean * rain7 + watertempmean	~pool_depth_mean + rain24 + day	3466.569	5.0250	0.0318	0.9468
~1	~day	~pool_depth_mean + rain24 + day	3468.404	6.8606	0.0127	0.9595
~1	~pool_depth_mean	~pool_depth_mean + rain24 + day	3469.114	7.5708	0.0089	0.9684
~1	~rain7	~pool_depth_mean + rain24 + day	3469.864	8.3204	0.0061	0.9745
~1	~pool_depth_mean + day	~pool_depth_mean + rain24 + day	3470.404	8.8606	0.0047	0.9792
~1	~rain7 + day	~pool_depth_mean + rain24 + day	3470.404	8.8606	0.0047	0.9839
~1	~watertempmean + day	~pool_depth_mean + rain24 + day	3470.404	8.8606	0.0047	0.9885
~1	~pool_depth_mean + rain7	~pool_depth_mean + rain24 + day	3470.476	8.9324	0.0045	0.9930
~1	~pool_depth_mean + watertempmean + day	~pool_depth_mean + rain24 + day	3472.404	10.8606	0.0017	0.9948
~1	~pool_depth_mean + rain7 + day	~pool_depth_mean + rain24 + day	3472.404	10.8606	0.0017	0.9965
~1	~pool_depth_mean * rain7	~pool_depth_mean + rain24 + day	3472.419	10.8755	0.0017	0.9982
~1	~pool_depth_mean * rain7 + day	~pool_depth_mean + rain24 + day	3473.153	11.6092	0.0012	0.9994
~1	~pool_depth_mean + rain7 + watertempmean + day	~pool_depth_mean + rain24 + day	3474.404	12.8606	0.0006	1.0000
~1	~1	~pool_depth_mean + rain24 + day	3495.759	34.2153	0.0000	1.0000

Note: As a Null model, a negative binomial model was taken, with constant parameters. AIC-weight, Δ and cumulative AIC weight were rounded to four decimal places. Asterisks indicate interactions. All models were calculated with se = F. For later estimations, models with Δ ≤ 2 were calculated once again. Note that these can deviate from this model selection, because of similar AIC values. Final models are highlighted in gray.

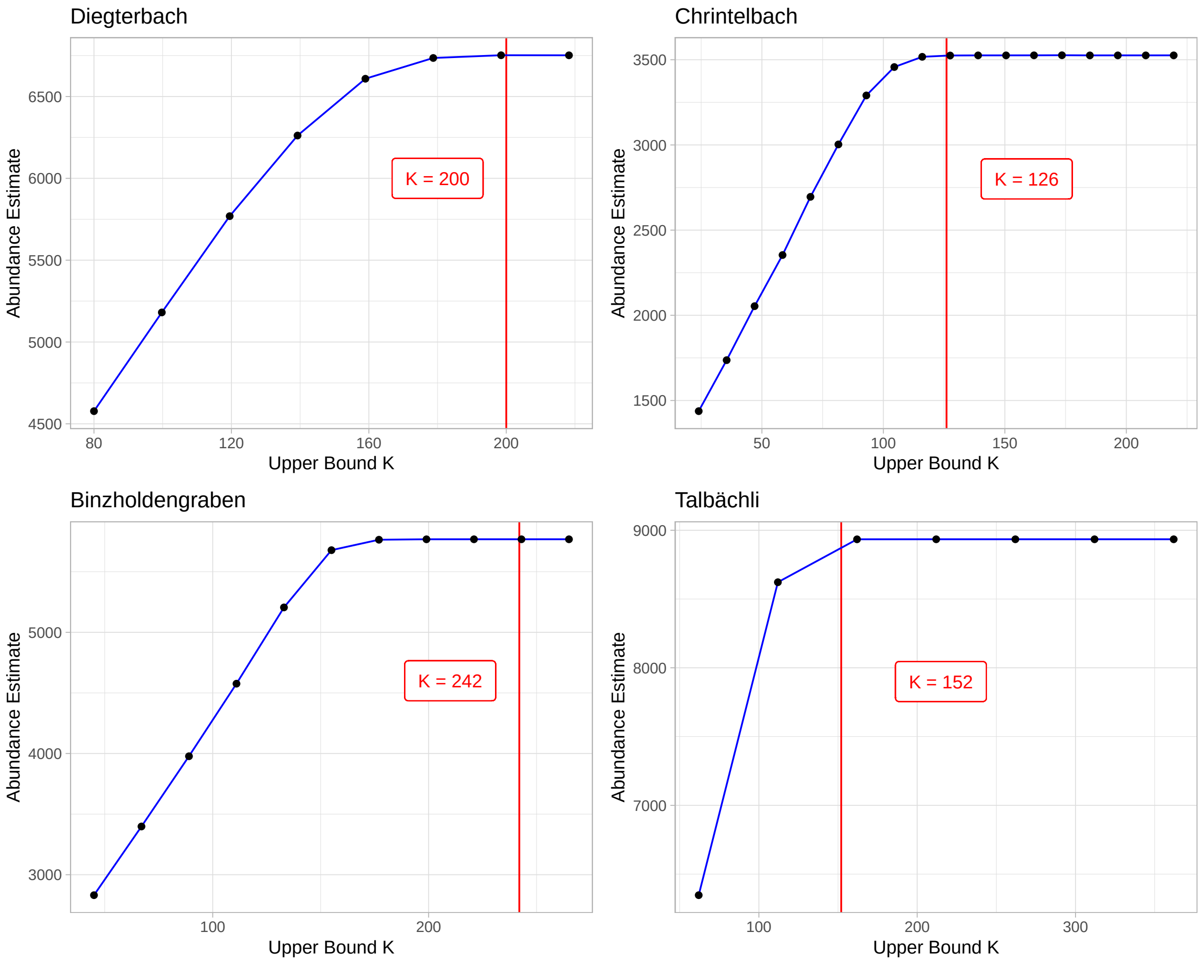

Figure 6: Manual selection of different upper bounds (K) with the help of an additional AIC values for each K. In red are the final K values, used for the respective model. These are based on a constant AIC value for with increasing value of K. Note, that there were not the same amount of K values modelled for each model since differences between streams were large and an increasing value of K increases the computation time massively.

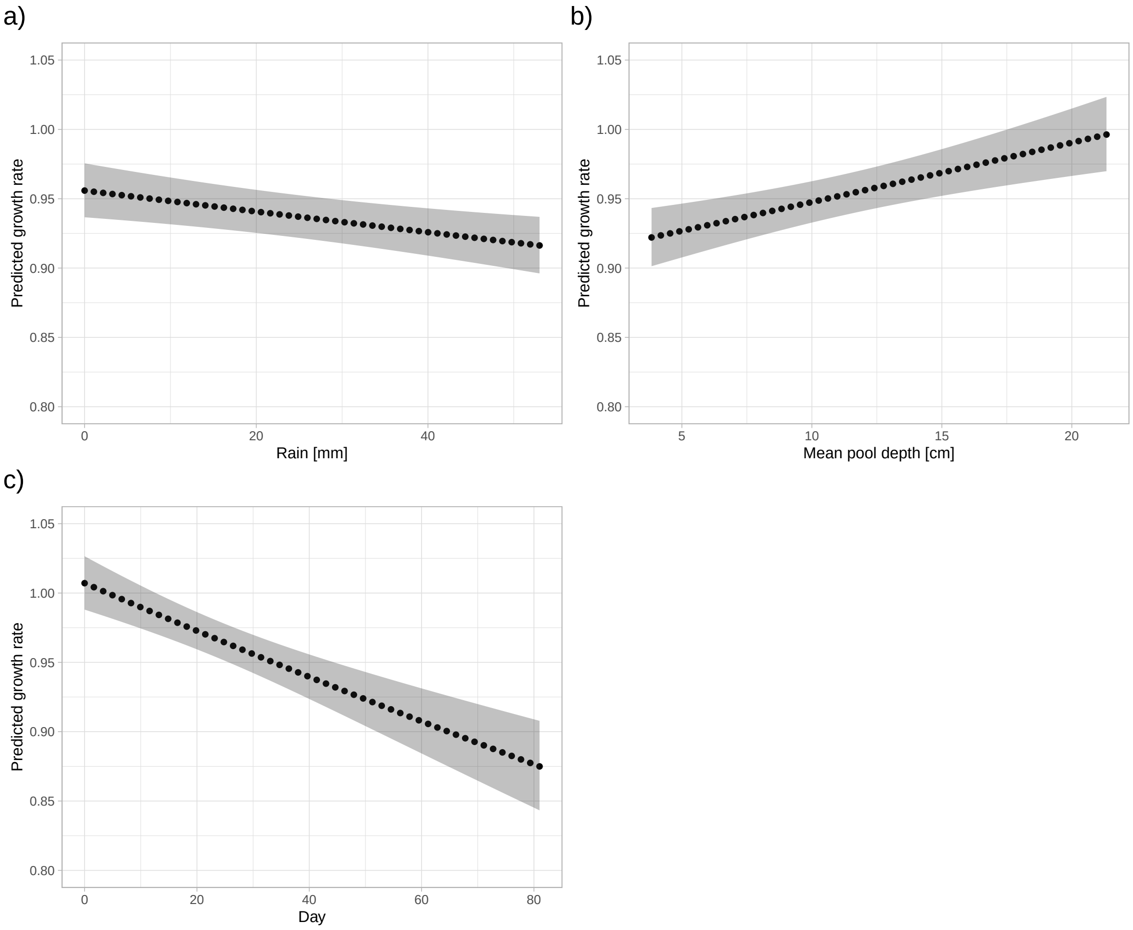

Figure 7: Predicted growth rate depending on a) rain, b) mean pool depth and c) day in stream Binzholdengraben.

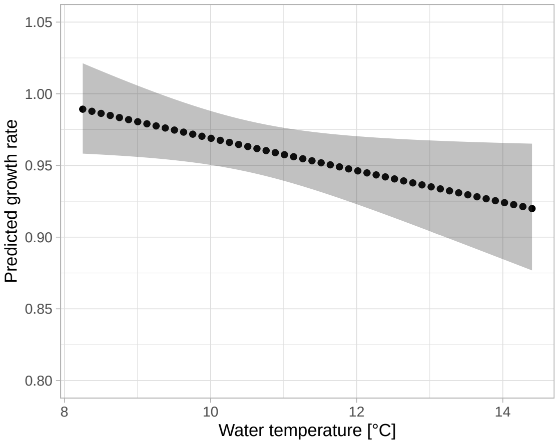

Figure 8: Predicted growth rate depending on water temperature in Chrintelbach.

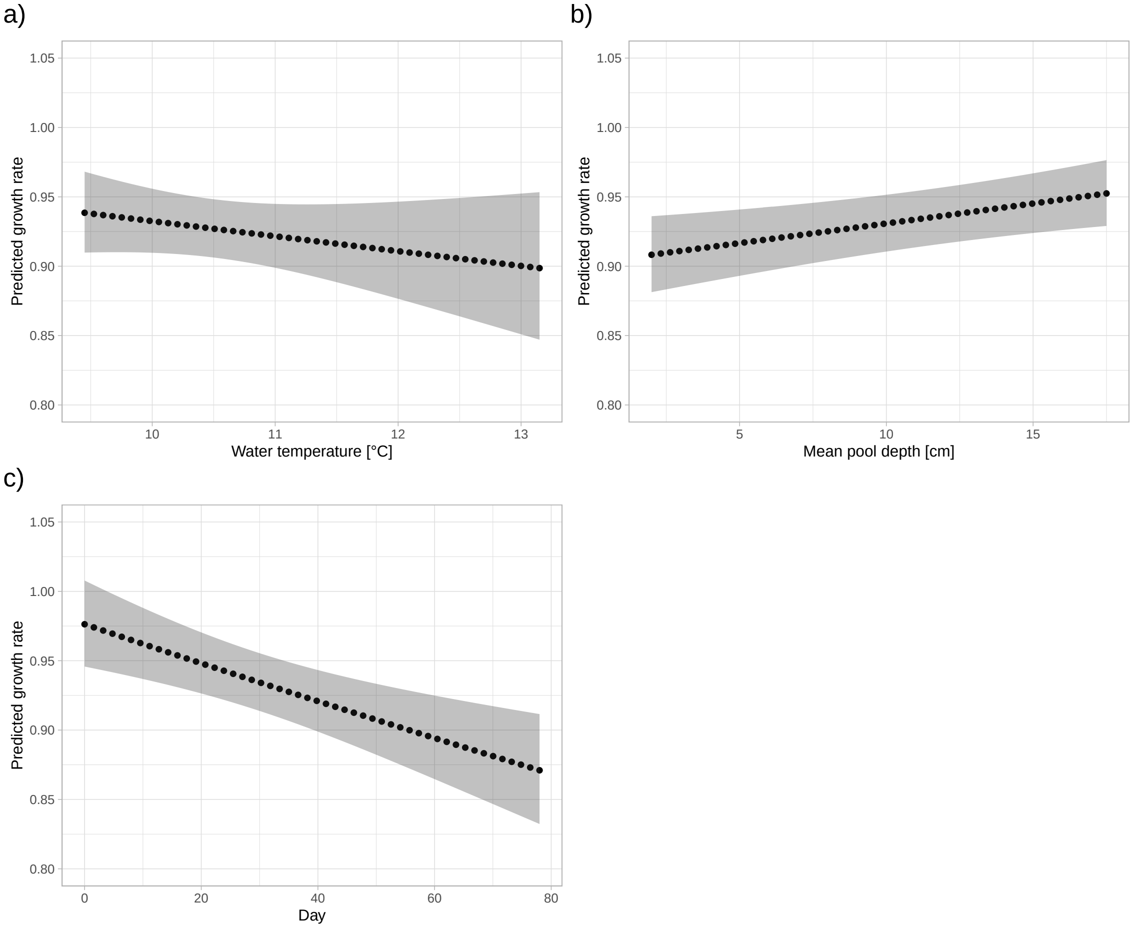

Figure 9: Predicted growth rate depending on a) water temperature, b) mean pool depth and c) day in stream Binzholdengraben.

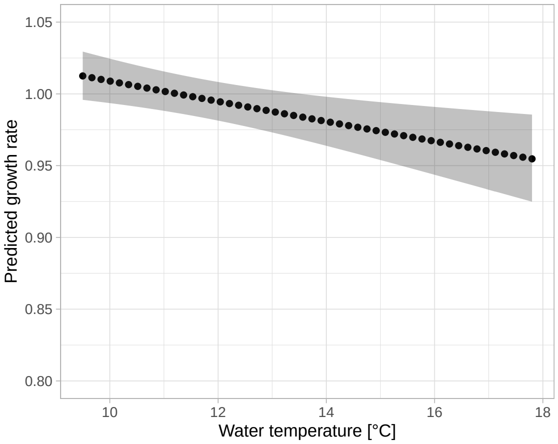

Figure 10: Predicted growth rate depending on water temperature in Talbächli.